International Journal of Engineering Trends and Technology
ISSN: 2231 – 5381 / https://doi.org/10.14445/22315381/IJETT-V71I2P235

Volume 71 Issue 2, 334-340, February 2023

Original Article

A Low-Cost IoT-Enabled Pyranometer; Based on the Peltier Element

M. Taha[1*], M. Omar[1], S. Khan[2], M. Usman[1], S. Larkin[3], M. Imran[2]

[1]*Technosense21, Islamabad, 44000, Pakistan*
[2]*National Transmission And Dispatch Company Limited, Islamabad, 44000, Pakistan*
[3]*Africa New Energies Limited, London, 533416, United Kingdom*

[1*]*Corresponding Author: taha@ts21.tech*

Received: 10 November 2022 Revised: 15 January 2023 Accepted: 18 February 2023 Published: 25 February 2023

Abstract *- Measurement of the intensity of solar irradiance is essential for designing renewable energy systems and atmospheric science. A low-cost, IoT-enabled pyranometer is proposed in this paper for data logging. The pyranometer is designed to measure the solar irradiance of spectral range from 300nm to 2800nm and hence covers UV, IR, and visible spectral ranges. The pyranometer exploits the phenomenon of thermoelectric sensing and photo sensing to measure solar irradiance. Peltier module TEC1-12706 with BPX65 silicon photodiode is used for this purpose. The combination of these sensors offers more precision in terms of diffused and direct solar irradiance. The open-circuit voltage Voc, cold, and hot side temperature of the Peltier are monitored to assess the solar irradiance. Also, the use of GPS and RTC module in the proposed system gives the exact location, time, and date of solar irradiance at a particular instant, which provides distinct features to the solution. The output signal is then processed through the microcontroller and transmitted to the cloud for analysis at the remote site.*

Keywords *- Pyranometer, IoT, Peltier, Irradiance, Sensor.*

1. Introduction

More than 95 % of the sun's energy is contained in the spectral range of 300nm to 2400nm [1]. The quantity of this radiation is referred to as global solar radiation or short-wave radiation. It is not easy to position environmental development on the planet driven directly or indirectly by solar energy.

Global measurements of sunlight are used in various applications for various targets. The solar panel's performance is primarily determined by solar energy because these panels convert solar energy into electricity [2].

Mainly, pyranometers are divided into two categories; Some measure the temperature rises of a black face against a thermal body or a reflecting white face, and some directly convert radiant energy to electrical energy like photometric types [3].

In thermo-electric sensor-based pyranometers, thermocouples are connected in series to get the temperature differential between active and cold junctions. This temperature differential produces an electromotive force linearly related to absorbed solar irradiance [4]. Although less expensive to produce, photometric types have spectrum responses defined by the semiconductor material, often silicon, and are not designated for reference-grade uses [5].

Irradiance readings with varying degrees of spectrum sensitivity will be produced depending on the type of pyranometer employed[6]. Variations in irradiance and temperature have various impacts on current and voltage in a solar panel[7].

In the case of irradiance, the current exhibits a more significant magnitude linear fluctuation than the voltage, although the voltage exhibits a logarithmic variation.

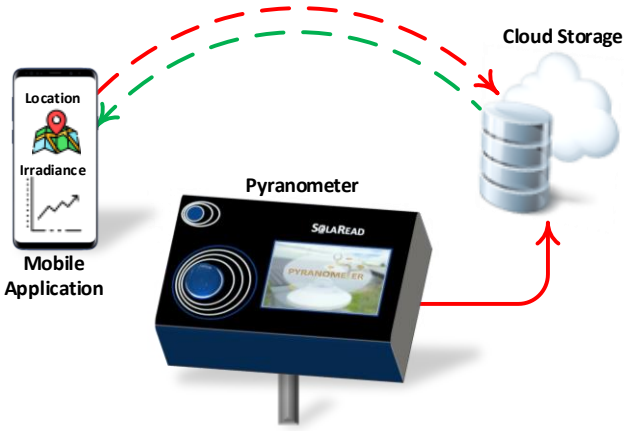

Fig. 1 Overview of the system.

On the other hand, temperature change has a more significant impact on voltage [8]. So, for the reliable measurement of solar radiations, thermo-electric-based pyranometers are preferable [9].

The proposed pyranometer based on the Peltier device determines a central data collection point over the cloud to store the data. Various sensors, including GPS, RTC, TEC1-12706, and photodiode, are used to assess and transmit real-time data to the cloud [10]. To monitor, the android application is used to fetch the data. In this way, concerned personnel stays informed regarding solar irradiance.

The paper focuses on the solar energy-based smart device embedded with the Wi-Fi module, which helps build a low-cost, low-power, and remote system. An overview of the system is illustrated in Figure 1. A few experiments have been performed to verify the results obtained with the designed system.

2. Proposed System

The overall block diagram of the suggested pyranometer is shown in Figure 2.

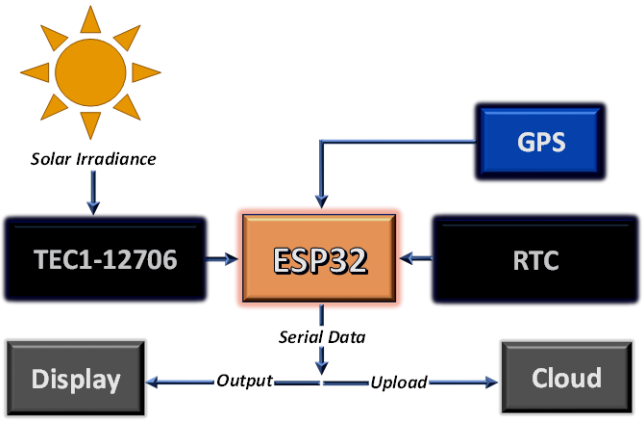

Fig. 2 Hardware architecture of the system.

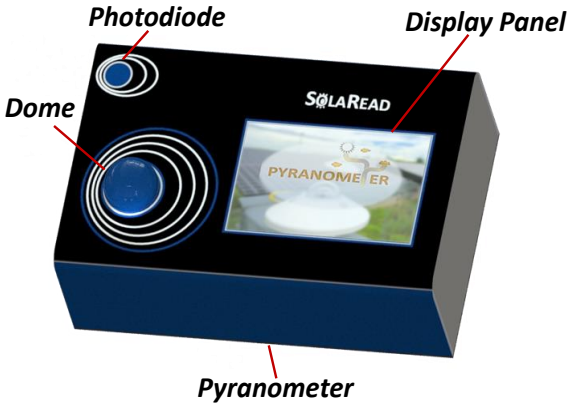

Fig. 3 3D model of the proposed IoT-enabled pyranometer.

This block diagram uses a Peltier module TEC1-12706 as a thermoelectric sensor. Black paint is applied to the hot surface of the Peltier module for low emissions. This painted side is exposed to solar light through a glass dome placed on a black acrylic box. A black-painted aluminium thermal sink is placed on the cold side of the Peltier module.

The thermal sink is helped to maintain the cold side at room temperature, and the acrylic box supports the thermal sink to maintain it at room temperature by protecting it from the external environment. The Peltier module chamber is separated from the electronics with the acrylic sheet so that the electronics' temperature will not disturb the Peltier module. The 3D model of the prototype of the IoT-enabled pyranometer is given in Figure 3. The prototype has its own display, which shows the real-time values of irradiance and location coordinates of the device.

The silica gel pack is used as a desiccant inside the chambers. When placed in sunlight, it maintains a temperature differential between the hot (black) surface and the cold surface of the Peltier module (TEC1-12706). It produces an electromotive force that has a comparatively lower value. The Peltier coefficient Π is defined as a ratio of the coefficient of thermal current Q to the coefficient of electric current I [11], as described in Equation 1.

$$Q = \Pi \, X \, I \qquad (1)$$

But it is not easy to measure the heat precisely compared to the temperature difference. So, using Onsager's Reciprocal Theorem, the Peltier coefficient Π can be calculated using the Seebeck coefficient, which is much easier to measure. Now the Peltier coefficient Π in terms of Seebeck coefficient S is [12] shown in Equation 2.

$$\Pi = S \, X \, T \qquad (2)$$

Here T is the temperature in a vacuum. For calculating the Seebeck coefficient S [13], an open circuit potential difference relation is used, as presented in Equation 3.

$$V_{oc} = S \, X \, (T_h - T_c) \qquad (3)$$

This electromotive force V_{oc} (open circuit potential difference) is directly proportional to the temperature differential $(T_h - T_c)$ and to the thermo-electric capability of the material, which is used as a sensor.

To measure the temperature of the cold side and hot side, two LM35 temperature sensors are used in this instrument. The open circuit voltage is first sent to 16-bit ADC and then towards the microcontroller for further processing. A BPX65 silicon pin photodiode is a low-cost photodiode used to measure direct visible light and increase the pyranometer's overall performance [14]. The luminance comparison of BPX65 with BPW20 [15] and BPW21 [16] is illustrated in Table 1.

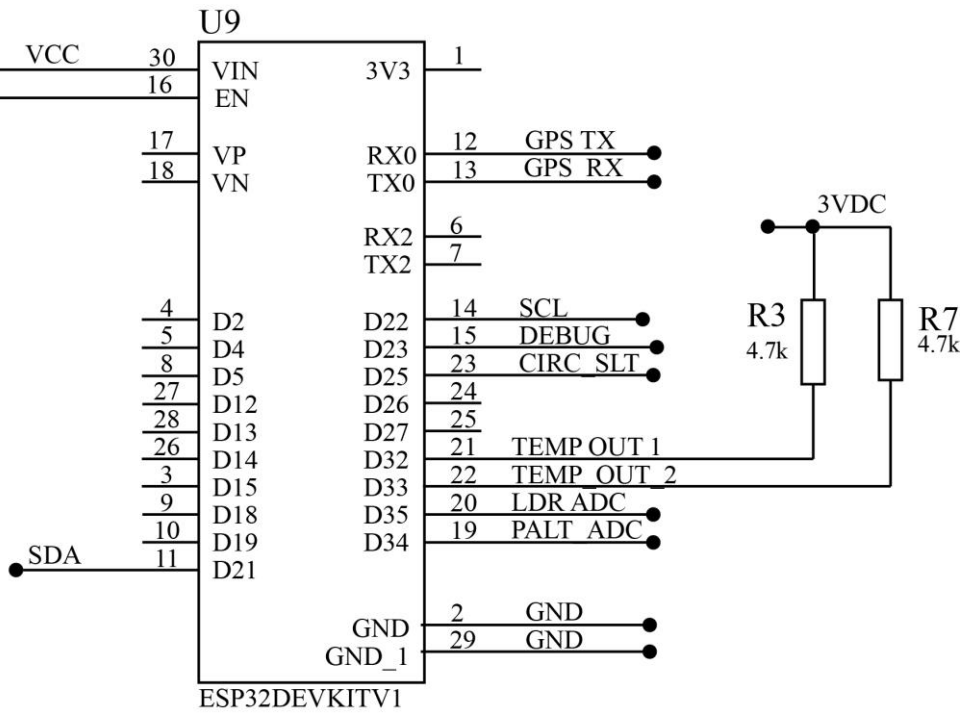

Fig. 4 Schematic diagram of ESP32 with various sensors in the proposed pyranometer

Table 1. Comparison of the produced voltages of different photodiodes w.r.t luminance

Lamp Volts (V)	Lumi-nance (Klux)	Output BPX65 (V)	Output BPW21 (V)	Output BPW20 (V)
0	0.11	0.55	0.6	0.59
15	2.8	1.01	0.75	1.07
22.5	118	1.92	1.59	2.3
27.8	232	2.76	2.6	3.4

A Neo 6M global positioning module is used for the location coordinates, and a tiny real-time clock is used to analyze the date and time of solar irradiance measurement. The geographical location, time, and solar irradiance values are then transmitted to the cloud by using an ESP32 microcontroller and can be retrieved through an android application.

3. Measurement Setup

The Pumped, major focus of this system is to build a low-cost with a wide spectral range monitoring system that can measure solar irradiance accurately.

The simulation of the proposed pyranometer includes the schematic diagram and the PCB layout of the pyranometer. The schematic and PCB layout are made up through *Proteus 8.9* and shown in Figures 4 and 5, respectively.

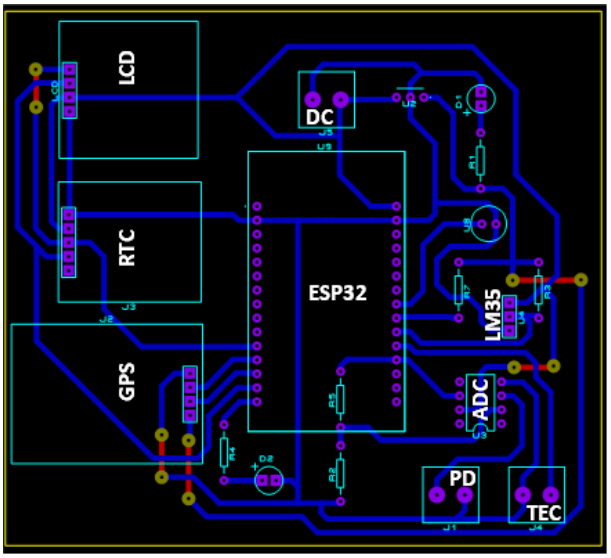

Fig. 5 PCB layout of proposed pyranometer.

The program of the microcontroller is finalized through the *Arduino IDE 1.8.7*. The measured values are then sent to ESP32 via serial communication. These measured values are further transmitted to the cloud and stored for analysis.

The flow diagram of the IoT-enabled pyranometer is given in Figure 6.

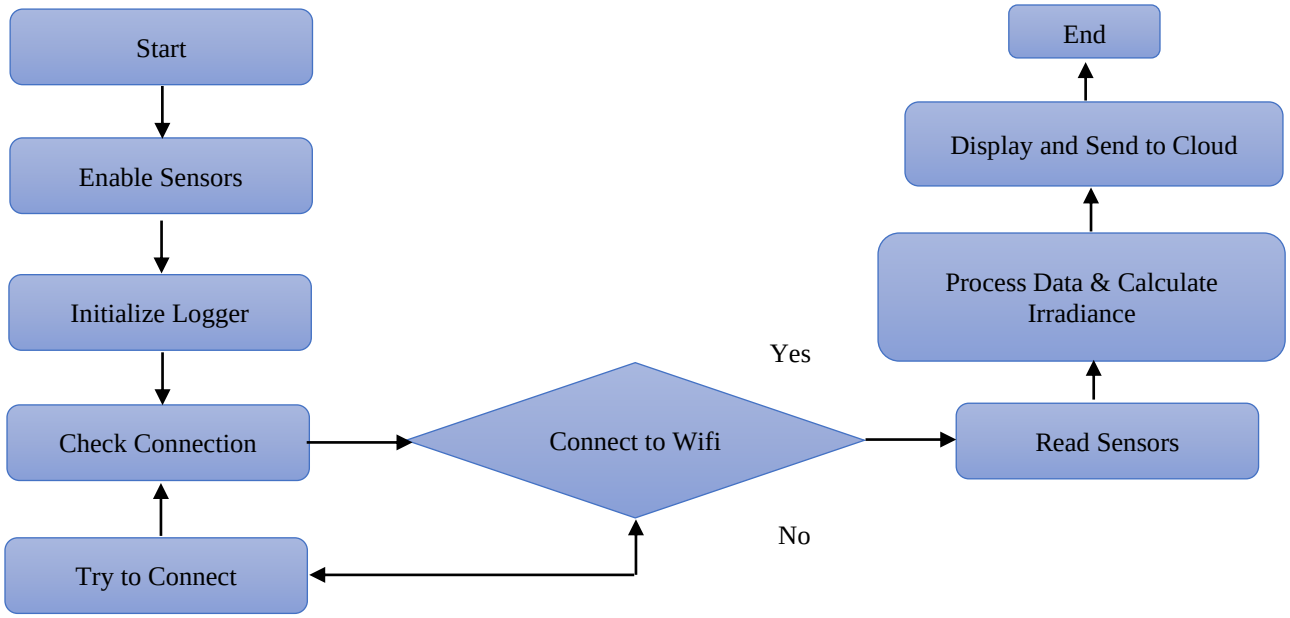

Fig. 6 Flow Diagram of the IoT- enabled Pyranometer

The sensing and processing of the proposed pyranometer are discussed in 3.1.

3.1. Experimental Conditions

The designed system efficiently measures solar irradiance using Peltier and photodiode. The data can be remotely accessed from the cloud by using a mobile application.

The experiment takes place in the laboratory with a 24W halogen light bulb [17]. The distance of the light source is changed in a PVC pipe so that the external environment does not interfere. The maximum distance of a light source from the Black painted hot side of the Peltier module is 50cm, which decreases as the experiment continues. Light intensity is measured through a digital light meter TES 1332A [18].

Photodiodes are a cheap replacement, and the only benefit in principle over thermoelectric sensors like Peltier in measuring irradiance, aside from their price, is their response time [19]. Since each wavelength in the solar spectrum has a distinct amplitude. Hence, no general conversion equation can be used to translate between lux and W/m2, and conversion is impossible without first knowing the spectral makeup of the light being measured [20].

In photodiode-based pyranometers, the response time is around 10µs compared to those based on thermoelectric sensors. The response time of thermoelectric sensors like Peltier ranges between 1 and 10s, making them less suitable for measuring swift changes in irradiance. The impact of temperature on pyranometer 0s measurement is also well known. However, this effect is lower in thermoelectric sensors-based pyranometers than in photodiode-based instruments [21].

The designed PCB of the suggested IoT-enabled pyranometer has both a Peltier device and a silicon photodiode. Various modules are integrated into PCB, as shown in Figure 7. Each module is connected to the ESP32 microcontroller. The TEC module and photodiode output are very low for the ESP32 microcontroller [22].

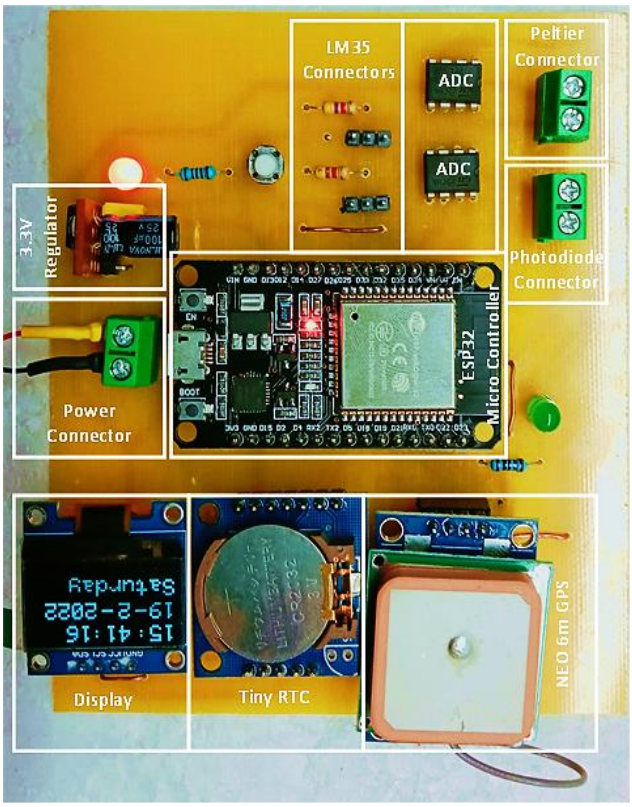

Fig. 7 Proposed hardware design of datalogger.

So, a 16-bit ADC is used to overcome this problem and can measure a change of 0.15mV if the reference voltage is 5V. This digital signal is then sent to the microcontroller for further processing and transmitted to the cloud.

3.2. Experimental Results

The plotted results of the sensed intensity of light values and measured distance of the light source are given in Figure 8. The plot shows the inverse relationship between the light intensity and the measured square of the distance between the source and the sensor surface when compared to ideally measured values. The proposed IoT-enabled pyranometer gave realistic results and was close to the ideal relationship.

The sensed temperature difference between the hot and cold surfaces of TEC1-12706 values through LM35 and measured light intensity values through a light meter are given in Figure 9. The plot shows the linear relationship between the light intensity and the temperature difference.

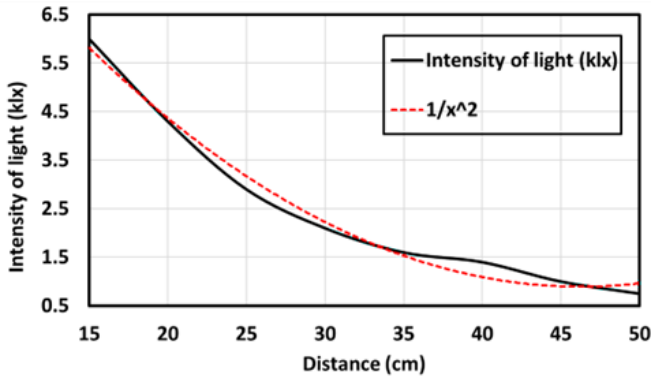

Fig. 8 Intensity of light vs the measured distance of the light source

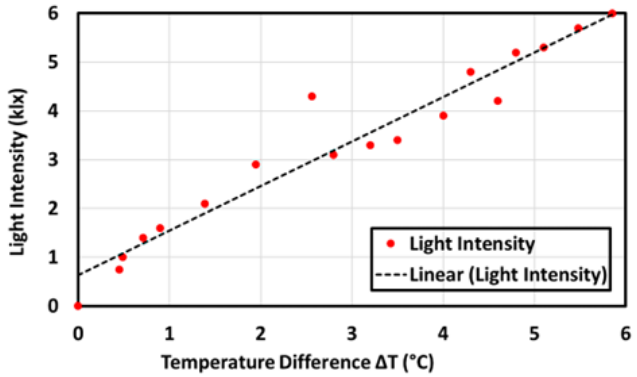

Fig. 9 Light intensity vs the temperature difference

The proposed pyranometer gave realistic results and was close to a straight line. Figure 10 shows the open-circuit voltage Voc measurements. The open circuit voltages are measured at different distances from the light source (halogen bulb) in the laboratory. The temperature is measured at the top face of the Peltier device. At the lowest distance, the change in temperature difference is maximum, hence the maximum open circuit voltages.

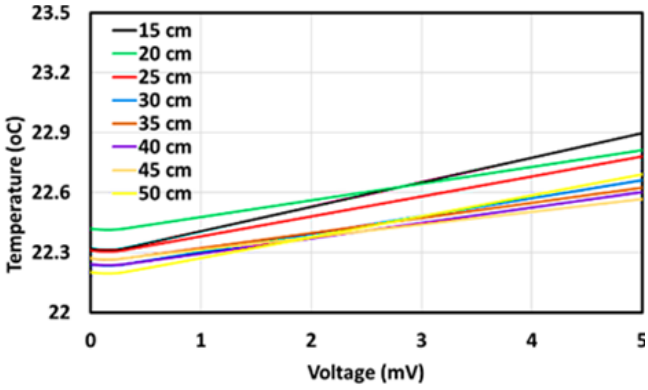

Fig. 10 Temperature vs open-circuit voltages Voc

Figure 11 shows the open circuit voltages Voc concerning the light intensity at that moment. The proposed system measures the voltage with the embedded sensors and gives satisfactory results. The open-circuit voltages increase if the light intensity increases and provide a linear relation.

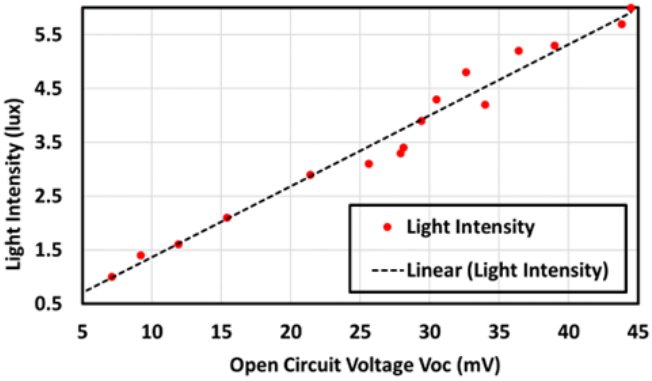

Fig. 11 Light intensity vs open-circuit voltages Voc.

The results are cross-checked with the overlapping band for the Peltier and the photosensor [23]. The relationship between irradiance and illuminance E_v for the spectrum is given in Equation 4 [24]:

$$E_v = k \int_{300}^{2800} V(\lambda) E(\lambda) d\lambda \qquad (4)$$

Here k is the conversion constant, V(ʎ) is the solar irradiance, and E(ʎ) is the illuminance data of an instrument. The subscript v (standing for "visible" or "visual") is written on photometric measures to differentiate them from radiometric measures. After evaluating all the controlled conditions and their results, the proposed system can be used in an external environment to measure the global horizontal irradiance.

3.3. Calibration and Results

The proposed pyranometer is calibrated and deployed for a full day at the location having coordinates of 33o40'52.5"N and 72o49'08.5"E.

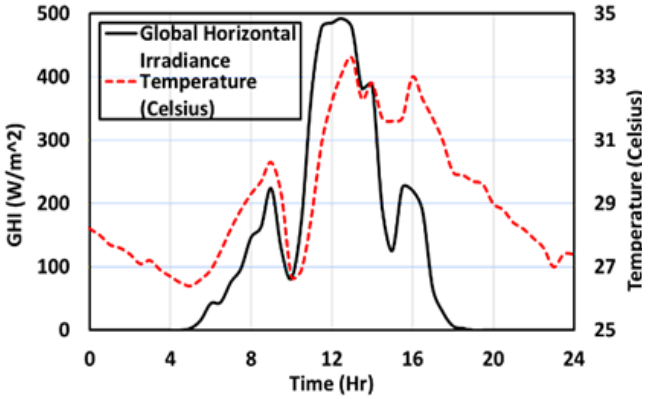

Fig. 12 Global horizontal irradiance and temperature vs local time.

Figure 12 illustrates the global horizontal irradiance and air temperature analysis concerning time.

The irradiance value is measured after 30 minutes on 3 Jul 2022. The proposed IoT-enabled pyranometer performs satisfactorily while measuring solar irradiance and temperature. The transient response of the pyranometer is described as an exponential decay characterized by a single time constant τ_c, and the error with respect to the final value is given in Equation 5 [6]:

$$\varepsilon(t) = e^{-t/\tau c} \qquad (5)$$

The time response of TEC1-12706 is approximately 13 sec, whereas the Kipp and Zonen have 2 sec. The rise time of temperature is faster compared to the fall time.

The experimental results give us good analytics. The technical methods used for measurement purposes proved to be effective and reliable. The microcontroller transmits the location, irradiance, and temperature concerning time to the cloud server.

Results retrieved from the cloud server can be displayed on the android to the user, causing simplicity in real-time solar irradiance monitoring. The android application can plot a graph of solar irradiance at a particular geographical location at any time.

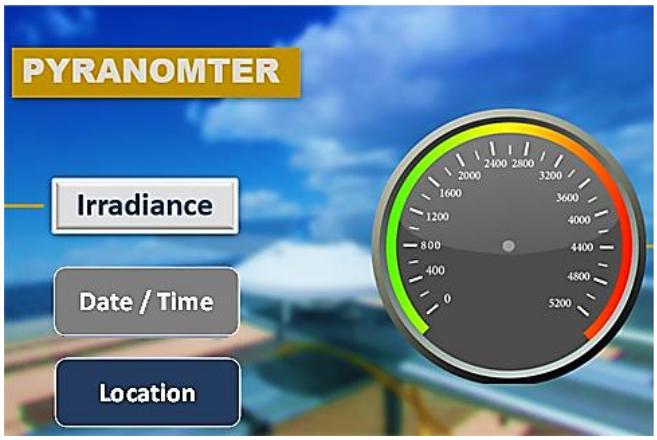

Fig. 13 GUI of the proposed android application

The Graphical User Interface (GUI) of the proposed android application is illustrated in Figure 13. The irradiance gauge represents the latest irradiance value, whereas the irradiance button opens a new tab representing the irradiance trend. Similarly, the date/time and location buttons give the time and coordinates of the position of the pyranometer.

4. Conclusion

This work uses a commercial module TEC1-12706 as a thermoelectric sensor and a photodiode to build a low-cost IoT-enabled pyranometer. The open-circuit voltage Voc and temperatures of Peltier's hot and cold sides are monitored to calculate the solar irradiance.

The microcontroller managed this pyranometer, and all the components were kept within the black box. The pyranometer's sensitivity was investigated, and the sensitivity was subsequently used to determine global irradiance within a spectral range of 300nm to 2800nm.

The proposed system is IoT-enabled, which helps monitor the data and transmit it promptly. An android application is intended to present real-time data at the user end with geographical location. This application also provides visual analytics of solar irradiance and temperature at any time.

References

[1] Muhammad Iqbal, *An Introduction to Solar Radiation*, Elsevier, 2012.

[2] Lawrence Dunn, Michael Gostein, and Keith Emery, "Comparison of Pyranometers vs. PV Reference Cells for Evaluation of PV Array Performance," *2012 38th IEEE Photovoltaic Specialists Conference*, pp. 002899-002904, 2012. *Crossref*, http://doi.org/10.1109/PVSC.2012.6318193

[3] Seun Oyelami et al., "A Pyranometer for Solar Radiation Measurement-Review," *Adeleke University Journal of Engineering and Technology*, vol. 3, no. 1, pp. 61-68, 2020.

[4] B Dieterink, CMP Serial Pyranometer 1007 AH Delft Netherlands, 2010. [Online]. Available: www.kippzonen.com

[5] K. Tohsing et al., "A Development of a Low-Cost Pyranometer for Measuring Broadband Solar Radiation," *Journal of Physics: Conference Series, IOP Publishing*, vol. 1380, p. 012045, 2019. *Crossref*, http://doi.org/10.1088/1742-6596/1380/1/012045

[6] Anton Driesse, "Radiometer Response Time and Irradiance Measurement Accuracy," *35th European Photovoltaic Solar Energy Conference and Exhibition*, pp. 1679-1683, 2018.

[7] Loredana Cristaldi et al., “A Simple Photovoltaic Panel Model: Characterization Procedure and Evaluation of the Role of Environmental Measurements,” *IEEE Transactions on Instrumentation and Measurement,* vol. 61, no. 10, pp. 2632-2641, 2012. *Crossref,* http://doi.org/10.1109/TIM.2012.2199196

[8] Yoshihiro Hishikawa et al., "Voltage-Dependent Temperature Coefficient of the I-V Curves of Crystalline Silicon Photovoltaic Modules," *IEEE Journal of Photovoltaics,* vol. 8, no. 1, pp. 48-53, 2018. *Crossref,* http://doi.org/10.1109/JPHOTOV.2017.2766529

[9] R. Guicherd, "Pyranometer for the Measurement of Solar Radiation," United States Patent US3876880A, 1975.

[10] E. Palo-Tejada et al., "Low-Cost Data Logging Device to Measure Irradiance Based on a Peltier Cell and Artificial Neural Network," *Journal of Physics: Conference Series*, vol. 1433, p. 012008, 2020. *Crossref,* http://doi.org/10.1088/1742-6596/1433/1/012008

[11] H. Julian Goldsmid, *The Seebeck and Peltier Effects,* The Physics of Thermoelectric Energy Conversion, Morgan & Claypool Publishers, 2017.

[12] Joshua Martin, Terry Tritt, and Ctirad Uher, "High Temperature Seebeck Coefficient Metrology," *Journal of Applied Physics*, vol. 108, no. 12, p. 14, 2010. *Crossref,* https://doi.org/10.1063/1.3503505

[13] Robert R. Heikes, and Roland W. Ure, *Thermoelectricity: Science and Engineering,* Interscience Publishers, 1961.

[14] O. O. Semiconductors, Silicon PIN Photodiode Version 1.3 BPX 65 - RS Components, 2015. [Online]. Available: www.osram-os.com

[15] I. Vishay Intertechnology, BPW20RF Silicon Photodiode, RoHS Compliant - Vishay, 2021. [Online]. Available: https://www.vishay.com/docs/81570/bpw20rf.pdf

[16] OSRAM Metal Can® TO39 Ambient Light Sensor, BPW 21, 2022. [Online]. Available: https://www.osram.com/ecat/com/en/class_pim_web_catalog_103489/prd_pim_device_2219533/

[17] Edward A Early, and Ambler Thompson, “Irradiance of Horizontal Quartz-Halogen Standard Lamps,” *Journal of Research of the National Institute of Standards and Technology*, vol. 101, no. 2, pp. 141-153, 1996. *Crossref,* https://doi.org/10.6028/jres.101.016

[18] I. I. LTD, TES-1330A/1332A/1334A Light Meter. [Online]. Available: https://btmco.ir/images/EditorUpload/TES%201330A.pdf

[19] K.L. Coulson, “Solar and Terrestrial Radiation,” Academic Press: New York, NY, USA, 1975.

[20] Pablo Casanaba, “Development of a Simple and Cheap Equipment for Monitoring the Solar Irradiance on PV Modules,” 2019.

[21] Simon Lineykin, and Shmuel Ben-Yaakov, "Modeling and Analysis of Thermoelectric Modules," *IEEE Transactions on Industry Applications*, vol. 43, no. 2, pp. 505-512, 2007. *Crossref,* https://doi.org/10.1109/TIA.2006.889813

[22] Renata I. S. Pereira et al., “IoT Network and Sensor Signal Conditioning for Meteorological Data and Photovoltaic Module Temperature Monitoring,” *IEEE Latin America Transactions*, vol. 17, no. 6, pp. 937-944, 2019. *Crossref,* https://doi.org/10.1109/TLA.2019.8896816

[23] Sameep Karki et al., "Performance Evaluation of Silicon-Based Irradiance Sensors Versus Thermopile Pyranometer," *IEEE Journal of Photovoltaics*, vol. 11, no. 1, pp. 144-149, 2021. *Crossref,* https://doi.org/10.1109/JPHOTOV.2020.3038342

[24] A Pons, A Barrio, and J Campos, “Variation of the Luminous Efficacy of Direct, Global, and Diffuse Solar Radiation with Atmospheric Parameters,” *Lighting Research Technology,* vol. 36, no. 1, pp. 31-43, 2004. *Crossref,* https://doi.org/10.1191/1477153504li102oa